

Novel Inhibitors of Neural Nitric Oxide Synthase Based on Inula Ssp. Compounds

Claudiu N. Lungu*

Department of Chemistry, Faculty of Chemistry and
Chemical Engineering, Babes-Bolyai University,
400028 Cluj

Constantinescu Teodora

Department of Chemistry, Faculty of Pharmacy, Iuliu
Hatieganu University, 400012Cluj Romania

Abstract:-Nitric oxide is a signaling molecule. Known as endothelium derived relaxing factor is biosynthesized from l-arginine, oxygen, and nicotinamide adenine dinucleotide phosphate by nitric oxide synthase enzymes. Inhibitors of nitric oxide synthase are thought as neuroprotective agents in traumatic brain injuries. Second derivative data from literature on a series of Inula spp. compounds with inhibitory activity on nitric oxide production were retrieved. Data were used for further research of nitric oxide synthase inhibitors. Computational strategies were used in order to bring together a hypothesis, further used in screening for pharmacologically active compounds with potential NO production inhibitory ability. A series of compounds resulted classified after docking energies and some drug like pharmacological filters. nNOS ligands interactions are described. Acceptor groups and carbonyl groups seems to be crucial in inhibiting nNOS.

Keywords:- Nitric oxide inhibition, nitric oxide synthase, blood brain barrier.

I. INTRODUCTION

Nitric oxide (NO) is involved in several pathologies, particularly in shock excessive NO production [1]. Inhibiting NO in such conditions was recognized improving the outcome[2]. Inhibiting NO production results in an increase in vascular pressure, with diminishing the inflammation. NO is involved in migraine, Parkinson disease and neural acute trauma[3]. In oncology, nitric oxide promotes tumor progression and metastasis[4]. Nitric oxide synthase is the main factor implied in NO production; it is an L-arginine based enzyme. Crystal structure of nitric oxid synthase (NOS) isoforms were consecutively elucidated: endothelial NOS (eNOS), inducible NOS (iNOS), and lastly in 2002 neuronal NOS (nNOS)[5]. NOS isoforms were validated as targets for new drugs, soon after their X-ray crystallography was available. Based on these, the design of effective and selective inhibitors has become an important approach in modern drug discovery involving NO biochemical pathways, related to dysfunctions of the human organism[6]. The objective of this study was to develop novel nNOS inhibitors starting from Inula spp. compounds witch were tested on RAW264.7. These are macrophage-like cells derived from Balbc mice. They keep many of the properties of macrophages including NO production, phagocytosis (beads, other), extreme sensitivity to TLR agonists and motility. They are susceptible to genetic drift so freezer stocks must be made from early passage number cells[7].

II. METHODS

To identify new compound with nNOS inhibitory ability, a structural-activity relationship hypothesis was first developed. In this respect, 52 compounds with IC₅₀ between 0.01 – 10.5 μM with inhibitory activity against NO production in LPS-simulated RAW264.7 cells were first considered. Two computational strategies were side by side used:(i) Propose a pharmacophore hypothesis, able to explain majority of activity; this hypothesis was then used for a virtual screening.(ii) Develop a QSAR (Quantitative Structure-Activity Relationship) in order to predict IC₅₀ and further explore structural relations between ligands and their bioactivity. A model using neural network regression was computed. It resulted a model with $r=0.966$, $r^2=0.991$, $p(\text{Spearman rank correlation})=0.990$, MSD (mean square deviation)=0.149, RMSD (root mean square deviation)=0.38646, $q^2(\text{cross validated square})=0.991$. Model regression equation is $y=0.987IC_{50} \text{ observed}+0.090$ (point 20.8 = 20.7735 was not detected as an outlier).

Regarding (i), to obtain a robust pharmacophore, other 42 Inula spp. compounds, without NO inhibitory properties, were considered. The concluding pharmacophore was derived using 42 inactive molecules and 52 active (IC₅₀=0.01-10.5 μM) ones. Pharmacophore features considered include hydrophobic centroids, aromatic rings, hydrogen bond acceptors and donors. Screening was performed using a commercially available data base[8].

Pharmacophore hypothesis, generated using 52 active compounds (Table 1) and 42 inactive compounds (Table 2) is shown in Figure 2.

Table1 Active compounds; IC50-half maximal inhibitory concentration(µM); S index-similarity index; arranged in ascending order of S index.

Compounds	IC50	S index
1	0.01	0
2	0.11	12.0513
3	5.6	12.4969
4	7.9	19.4699
5	6.9	22.3426
6	9.5	25.5101
7	5.3	27.5709
8	0.11	29.0629
9	0.13	29.0802
10	7.9	31.3892
11	1.1	39.3352
12	8.4	40.1091
13	10.5	40.6126
14	0.11	42.1873
15	3.5	47.3375
16	6.35	61.6194
17	3.5	66.1759
18	2.45	72.7035
19	7	76.7985
20	7.2	76.817
21	3.2	77.8637
22	5.39	81.9833
23	0.6	92.5224
24	6.3	92.7287
25	8	92.8649
26	7.9	101.613
27	0.013	101.803
28	0.1	102.129
29	9.2	103.314
30	9.8	103.37
31	8.2	103.601
32	5.1	150.325
33	7.3	162.822
34	0.46	249.564
35	3.9	249.983
36	3.8	274.82
37	0.25	313.36
38	3.5	313.38
39	2.2	322.92
40	9.9	323.056
41	6.6	333.059
42	6.4	396.632
43	1.5	480.777
44	0.11	783.961
45	2.2	807.76
46	1.59	3565.76
47	1.52	3696.54
48	4.1	3764.74
49	20.8	4040.21
50	12	4191.84
51	4.5	5498.53
52	9.6	5860.64

Table2 Inactive compounds. MW-molecular weight . S index-similarity index. Arrange in ascending order in respect to similarity index.

Compounds	MW	S index
1	232.318	0
2	232.318	30.15
3	234.334	38.2493
4	234.334	4.48171
5	234.334	4.59192
6	238.28	24.2974
7	248.317	71.2268
8	248.317	56.6423
9	248.317	109.454
10	248.317	62.4100
11	248.317	52.7517
12	248.317	85.4745
13	250.333	194.314
14	250.333	164.608
15	252.306	86.7258
16	254.322	176.044
17	280.316	340.867
18	286.236	450.48
19	286.239	462.272
20	290.354	388.531
21	296.403	502.604
22	302.279	555.264
23	306.354	485.076
24	306.354	485.084
25	306.354	508.831
26	316.262	709.786
27	316.262	678.025
28	322.353	561.653
29	330.289	798.709
30	338.295	916.648
31	344.315	947.263
32	346.288	973.308
33	350.406	793.172
34	362.46	1183.6
35	364.433	1112.36
36	396.432	1463.61
37	398.664	1523.09
38	416.507	2196.38
39	448.377	2232.92
40	480.548	2468.05
41	516.451	4499.49
42		

2.0 fs, frame interval 10fs, 10000 steps termination, heat cooling rate 1.000kcal/atom/ps, target temperature 301.15K. Model equation was used to predict IC50 for compounds remaining after the screening using the best suited pharmacophore hypothesis. Descriptors used in the model building are: H -atoms number, O-atoms number, Csp3(3??)-number of sp3 hybridized C-atom, carbonyl- number of carbonyl groups, Et -number of ether groups, Ha-Ha-min - minimal distance between 2 hydrogen acceptor groups, HA-HA-mean- average distance between two hydrogen acceptor groups. Descriptors composing the model were analyzed by Tolerance and Value of Inflation. A tolerance <0.20[12] and a VIF>10[13].Hydrogen acceptor groups and carbonyl groups seems to be crucial in inhibiting nNOS.

Table 3 Descriptors composing model Tolerance and Value of inflation (VIF)

Nr	Descriptor	r2	Tolerance(1-r2)	VIF 1/(1-r2)
1	2HA min	0.255814	0.744186	1.34375
2	CO	0.72975	0.27025	3.700278
3	2Ha average	0.769236	0.230764	4.333432
4	Et	0.894086	0.105914	9.441622
5	O	0.916796	0.083204	12.01865
6	Csp3	0.959513	0.040487	24.69929
7	H	0.964551	0.035449	28.20954

Several hypotheses were analyzed: a three future hypothesis AAH explains 90% of activity. Pharmacophore is shown in Figure 2;a four future pharmacophore AAHH explains 80% of activity; a five future pharmacophore AAAHH explains 60% of activity.

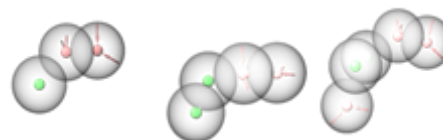


Fig 2:- AAH : H x0.45 y0.16 z 0.11 Ax -0.45 y -0.21 z 2.90 A x -2.06 y -1.50 z 3.89 AAHH : H x -1.06 y 1.44 z -0.80 H x -0.22 y -0.37 z 0.27 A x -1.12 y -0.75 z 3.06 A x -2.73 y -2.03 z 4.06; AAAHH A x -1.11 y 0.97 z -3.32 H x -0.35 y 2.08 z -0.55 H x 0.53y 0.31 y 0.26 A x -0.39 y -0.13 z 3.02 A x -1.97 y -1.46 z 3.99; (green-hydrophobic, red – acceptor);

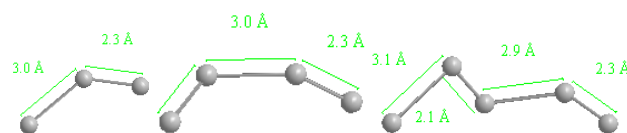


Fig 3:- Pharmacophore hypothesis drawn using Cartesian coordinates: (from a to c) AAH, AAHH and AAAHH hypothesis respectively. AAH distance atoms (2)-(3) 2.288Å,(1)-(2)2.955Å; angle (3)-(2)-(1) 133.899Å. AAHH distance atoms (3)-(4)2.287Å, (2)-(3)2.956Å, (1)-(2)2.264Å; angle(4)-(3)-(2)134.343Å, (3)-(2)-(1)115.838Å; dihedral angle (1)-(2)-(3)-(4)97.880Å. AAAHH distance atoms (4)-(5)2.282Å, (3)-(4)2.942Å, (2)-(3)2.136Å, (1)-(2)3.079Å; angle(5)-(4)-(3)134.624Å, (4)-(3)-(2)110.535Å, (3)-(2)-(1)98.284Å; dihedral angle (2)-(3)-(4)-(5)99.718Å, (1)-(2)-(3)-(4)-135.606Å.

Furthermore, a molecular dynamic statistical study[9] was performed on pharmacophore hypothesis[10] by considering each hypothetical atom as a Carbon atom and representing the particular hypothesis as a C-atom chain. Tinker software package[11] was used in this respect. Molecular dynamics parameters were as follows: step interval

Concerning (ii), a similarity score based selection was performed. Only active compounds were considered. Data set was divided into a training set and a test set. Molecules were

ordered by the similarity score using as similarity template OC(C1)C2C(=C)C(=O)OC2C3OC3(C)CCC=C1 having the lowest IC₅₀ (0.01 μM);the first 26 results were taken, in IC₅₀ ascending order. Model was built using multiple linear regression[12] (MLR). Descriptors used to build the model were: H, C, N, O,P,S atoms, molecular weight (MW), total number of atoms, number of heavy atoms, number of rotational bounds, number of hydrogen donor groups (HD), number of hydrogen accepting groups (HA), number of rings, minimal distance between two hydrogen donor groups, maximal distance between two hydrogen donor groups, minimal distance between two hydrogen accepting groups, maximal distance between two hydrogen accepting groups, aromaticity (Aro). In order to correlate model data with nNOS, docking was performed; the binding energy (kcal/mol) nNOS-ligand was introduced in the QSAR model. A further selection was done to keep the proper descriptors. Model was internally validated by the leave-one-out technique and externally, using the test set data. The descriptors used in the model were finally selected by evaluating their variance, tolerance and interrelationship.

The result on IC₅₀% explanation by MD pharmacophore AAHH hypothesis was used for screening (over 11.000 hits) in a data base applying the filters discussed in Methods section. Resulted screening compounds were classified after docking energies (see Table 5) as discussed in the Methods section. The best 42 compounds binding energies were discussed (the remaining data are shown in Supplementary materials).

A second screening was performed applying the pharmacological filters: molecular weight (390-420g/mol), partition coefficient xlogP (1-3), number of rotatable bounds (4-6), hydrogen bound donors (2-4), hydrogen bond acceptors (4-6). Filters characterizing solvent interaction were also used: apolar desolvation (0-10 kcal/mol) and polar desolvation(-40-0 kcal/mol). Membrane permeation was also considered: polar surface area was limited at 60-80 Å² and the net charge of a molecule was set zero. The IC₅₀ of remaining 21 molecules was then predicted by a QSAR model.

III. RESULTS

Pharmacophore hypothesis, generated using 52 active compounds (Table 1) and 42 inactive compounds (Table 2) is shown in Figure 2.

Table1 Active compounds; IC50 -half maximal inhibitory concentration(μM); S index-similarity index; arranged in ascending order of S index.

Compounds	IC50	S index	
1	OC(C1)C2C(=C)C(=O)OC2C3OC3(C)CCC=C1	0.01	0
2	O=C1OC2C3OC3(C)CCC=C1C	0.11	12,0513
3	O=C1OC2C3OC3(C)CCC=C1C	5.6	12,4969
4	O=C1OC2C3OC3(C)CCC=C1C	7.9	19,4699
5	O=C1OC2C3OC3(C)CCC=C1C	6.9	22,3426
6	O=C1OC2C3OC3(C)CCC=C1C	9.5	25,5101
7	O=C1OC2C3OC3(C)CCC=C1C	5.3	27,5709
8	O=C1OC2C3OC3(C)CCC=C1C	0.11	29,0629
9	O=C1OC2C3OC3(C)CCC=C1C	0.13	29,0802
10	O=C1OC2C3OC3(C)CCC=C1C	7.9	31,3892
11	O=C1OC2C3OC3(C)CCC=C1C	1.1	39,3352
12	O=C1OC2C3OC3(C)CCC=C1C	8.4	40,1091
13	O=C1OC2C3OC3(C)CCC=C1C	10.5	40,6126
14	O=C1OC2C3OC3(C)CCC=C1C	0.11	42,1873
15	O=C1OC2C3OC3(C)CCC=C1C	3.5	47,3375
16	O=C1OC2C3OC3(C)CCC=C1C	6.35	61,6194
17	O=C1OC2C3OC3(C)CCC=C1C	3.5	66,1759
18	O=C1OC2C3OC3(C)CCC=C1C	2.45	72,7035
19	O=C1OC2C3OC3(C)CCC=C1C	7	76,7985
20	O=C1OC2C3OC3(C)CCC=C1C	7.2	76,817
21	O=C1OC2C3OC3(C)CCC=C1C	3.2	77,8637
22	O=C1OC2C3OC3(C)CCC=C1C	5.39	81,9833
23	O=C1OC2C3OC3(C)CCC=C1C	0.6	92,5224
24	O=C1OC2C3OC3(C)CCC=C1C	6.3	92,7287
25	O=C1OC2C3OC3(C)CCC=C1C	8	92,8649
26	O=C1OC2C3OC3(C)CCC=C1C	7.9	101,613
27	O=C1OC2C3OC3(C)CCC=C1C	0.013	101,803
28	O=C1OC2C3OC3(C)CCC=C1C	0.1	102,129
29	O=C1OC2C3OC3(C)CCC=C1C	9.2	103,314
30	O=C1OC2C3OC3(C)CCC=C1C	9.8	103,37
31	O=C1OC2C3OC3(C)CCC=C1C	8.2	103,601
32	O=C1OC2C3OC3(C)CCC=C1C	5.1	150,325
33	O=C1OC2C3OC3(C)CCC=C1C	7.3	162,827
34	O=C1OC2C3OC3(C)CCC=C1C	0.46	249,564
35	O=C1OC2C3OC3(C)CCC=C1C	3.9	249,983
36	O=C1OC2C3OC3(C)CCC=C1C	3.8	274,82
37	O=C1OC2C3OC3(C)CCC=C1C	0.25	313,36
38	O=C1OC2C3OC3(C)CCC=C1C	3.5	313,38
39	O=C1OC2C3OC3(C)CCC=C1C	2.2	322,92
40	O=C1OC2C3OC3(C)CCC=C1C	9.9	323,056
41	O=C1OC2C3OC3(C)CCC=C1C	6.6	333,059
42	O=C1OC2C3OC3(C)CCC=C1C	6.4	396,632
43	O=C1OC2C3OC3(C)CCC=C1C	1.5	480,777
44	O=C1OC2C3OC3(C)CCC=C1C	0.11	783,961
45	O=C1OC2C3OC3(C)CCC=C1C	2.2	807,76
46	O=C1OC2C3OC3(C)CCC=C1C	1.59	3565,76
47	O=C1OC2C3OC3(C)CCC=C1C	1.52	3696,54
48	O=C1OC2C3OC3(C)CCC=C1C	4.1	3764,74
49	O=C1OC2C3OC3(C)CCC=C1C	20.8	4040,21
50	O=C1OC2C3OC3(C)CCC=C1C	12	4191,84
51	O=C1OC2C3OC3(C)CCC=C1C	4.5	5498,53
52	O=C1OC2C3OC3(C)CCC=C1C	9.6	5860,64

Table2 Inactive compounds, MW- molecular weight , S index-similarity index. Arrange in ascending order in respect to similarity index.

Compounds	MW	S index	
1	O=C1OC2C3OC3(C)CCC=C1C	232,318	0
2	O=C1OC2C3OC3(C)CCC=C1C	232,318	30,15
3	O=C1OC2C3OC3(C)CCC=C1C	234,334	38,2493
4	O=C1OC2C3OC3(C)CCC=C1C	234,334	4,48171
5	O=C1OC2C3OC3(C)CCC=C1C	234,334	4,59192
6	O=C1OC2C3OC3(C)CCC=C1C	238,28	24,2974
7	O=C1OC2C3OC3(C)CCC=C1C	248,317	71,4288
8	O=C1OC2C3OC3(C)CCC=C1C	248,317	56,6423
9	O=C1OC2C3OC3(C)CCC=C1C	248,317	109,454
10	O=C1OC2C3OC3(C)CCC=C1C	248,317	62,4100
11	O=C1OC2C3OC3(C)CCC=C1C	248,317	52,7517
12	O=C1OC2C3OC3(C)CCC=C1C	248,317	85,745
13	O=C1OC2C3OC3(C)CCC=C1C	250,333	194,314
14	O=C1OC2C3OC3(C)CCC=C1C	250,333	164,608
15	O=C1OC2C3OC3(C)CCC=C1C	252,306	86,7258
16	O=C1OC2C3OC3(C)CCC=C1C	254,322	176,044
17	O=C1OC2C3OC3(C)CCC=C1C	280,316	340,867
18	O=C1OC2C3OC3(C)CCC=C1C	286,236	450,48
19	O=C1OC2C3OC3(C)CCC=C1C	286,279	462,272
20	O=C1OC2C3OC3(C)CCC=C1C	290,358	388,531
21	O=C1OC2C3OC3(C)CCC=C1C	296,403	502,604
22	O=C1OC2C3OC3(C)CCC=C1C	302,279	555,264
23	O=C1OC2C3OC3(C)CCC=C1C	306,354	485,076
24	O=C1OC2C3OC3(C)CCC=C1C	306,354	485,084
25	O=C1OC2C3OC3(C)CCC=C1C	306,354	508,831
26	O=C1OC2C3OC3(C)CCC=C1C	316,262	709,786
27	O=C1OC2C3OC3(C)CCC=C1C	316,262	678,025
28	O=C1OC2C3OC3(C)CCC=C1C	322,353	561,653
30	O=C1OC2C3OC3(C)CCC=C1C	330,289	798,709
31	O=C1OC2C3OC3(C)CCC=C1C	338,395	916,648
32	O=C1OC2C3OC3(C)CCC=C1C	344,315	947,263
33	O=C1OC2C3OC3(C)CCC=C1C	346,288	973,308
34	O=C1OC2C3OC3(C)CCC=C1C	350,408	793,172
35	O=C1OC2C3OC3(C)CCC=C1C	362,46	1183,6
36	O=C1OC2C3OC3(C)CCC=C1C	364,433	1112,56
37	O=C1OC2C3OC3(C)CCC=C1C	396,432	1463,61
38	O=C1OC2C3OC3(C)CCC=C1C	398,664	1523,09
39	O=C1OC2C3OC3(C)CCC=C1C	416,507	2196,38
40	O=C1OC2C3OC3(C)CCC=C1C	448,377	2237,92
41	O=C1OC2C3OC3(C)CCC=C1C	480,548	2468,05
42	O=C1OC2C3OC3(C)CCC=C1C	516,451	4499,49

QSAR model was computed. Descriptors used for building the model were discussed in the Method section. In order to improve the model, principal components were computed for each descriptor. A model using neural network regression was computed. It resulted a model with r=0.966, r²=0.991, p(Spearman rank correlation)=0.990, MSD (mean square deviation)=0.149, RMSD (root mean square

deviation)=0.38646, q^2 (cross validated square)=0.991. Model regression equation is $y=0.9871C_{50}$ observed+0.090 (point 20.8 = 20.7735 was not detected as an outlier).

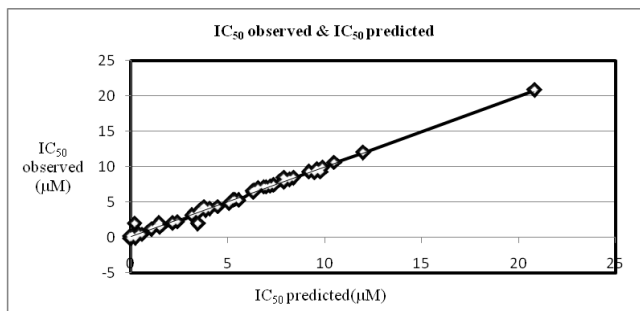


Fig 4:- Plot representing correlation between observed and predicted IC₅₀ values.

Model equation was used to predict IC₅₀ for compounds remaining after the screening using the best suited pharmacophore hypothesis. Descriptors used in the model building are: H -atoms number, O-atoms number, Csp³-number of sp³ hybridized C-atom, carbonyl- number of carbonyl groups, Et -number of ether groups, Ha-Ha-min - minimal distance between 2 hydrogen acceptor groups, HA-HA-mean- average distance between two hydrogen acceptor groups. Descriptors composing the model were analyzed by Tolerance and Value of Inflation. A tolerance <0.20[12] and a VIF>10[13].Hydrogen acceptor groups and carbonyl groups seems to be crucial in inhibiting nNOS.

Nr	Descriptor	r2	Tolerance(1-r2)	VIF 1/(1-r2)
1	2HA min	0.255814	0.744186	1.34375
2	CO	0.72975	0.27025	3.700278
3	2Ha average	0.769236	0.230764	4.333432
4	Et	0.894086	0.105914	9.441622
5	O	0.916796	0.083204	12.01865
6	Csp ³	0.959513	0.040487	24.69929
7	H	0.964551	0.035449	28.20954

Several hypotheses were analyzed: a three future hypothesis AAH explains 90% of activity. Pharmacophore is shown in Figure 2;a four future pharmacophore AAHH explains 80% of activity; a five future pharmacophore AAAHH explains 60% of activity.

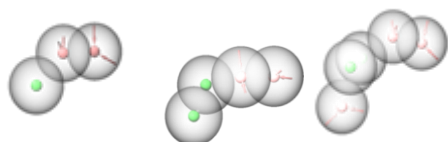


Fig 2:- AAH : H x0.45 y0.16 z 0.11 Ax -0.45 y -0.21 z 2.90 A x -2.06 y -1.50 z 3.89 AAHH : H x -1.06 y 1.44 z -0.80 H x -0.22 y -0.37 z 0.27 A x -1.12 y -0.75 z 3.06 A x -2.73 y -2.03 z 4.06; AAAHH A x -1.11 y 0.97 z -3.32 H x -0.35 y 2.08 z -0.55H x 0.53y 0.31 y 0.26 A x -0.39 y -0.13 z 3.02 A x -1.97 y -1.46 z 3.99; (green-hydrophobic, red – acceptor);

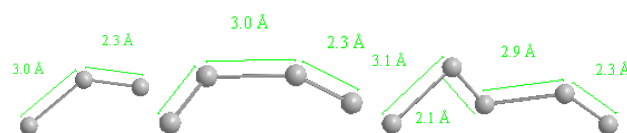


Fig 3:-Pharmacophore hypothesis drawn using Cartesian coordinates: (from a to c) AAH, AAHH and AAAHH hypothesis respectively. AAH distance atoms (2)-(3)2.288Å,(1)-(2)2.955Å; angle (3)-(2)-(1) 133.899Å. AAHH distance atoms (3)-(4)2.287Å, (2)-(3)2.956Å, (1)-(2)2.264Å; angle(4)-(3)-(2)134.343Å, (3)-(2)-(1)115.838Å; dihedral angle (1)-(2)-(3)-(4)97.880Å. AAAHH distance atoms (4)-(5)2.282Å, (3)-(4)2.942Å, (2)-(3)2.136Å, (1)-(2)3.079Å;angle(5)-(4)-(3)134.624Å,(4)-(3)-(2)110.535Å,(3)-(2)-(1)98.284Å; dihedral angle (2)-(3)-(4)-(5)99.718Å, (1)-(2)-(3)-(4)-135.606Å.

MD analysis[14] of all the three pharmacophores showed that hypothesis AAHH has the smallest SD values for three points (Table 3: AAH 5.444, AAHH 5.053, AAAHH 5.106). Lowest SD correlates with low variability i.e low spatial geometric variability. Low geometric variability results in pharmacophore futures-properties conservation.

Pharmacophore	Measurement	min	max	average	SD
AAH	C(2)-C(3)	1.426	1.678	1.542	0.037
	C(1)-C(2)	1.428	1.680	1.542	0.037
	C(1)-C(2)-C(3)	99.222	127.143	112.520	5.444
AAHH	C(3)-C(4)	1.434	1.681	1.543	0.037
	C(3)-C(2)	1.424	1.700	1.547	0.040
	C(2)-C(1)	1.429	1.706	1.542	0.037
	C(2)-C(3)-C(4)	98.481	127.474	113.720	4.935
	C(3)-C(2)-C(1)	99.455	128.729	113.675	5.053
AAAHH	C(4)-C(3)-C(2)-C(1)	-179.665	179.992	58.176	62.629
	C(5)-C(4)	1.441	1.667	1.542	0.033
	C(4)-C(3)	1.440	1.696	1.546	0.035
	C(2)-C(3)	1.449	1.677	1.546	0.034
	C(2)-C(1)	1.438	1.672	1.542	0.035
	C(5)-C(4)-C(3)	99.454	130.096	114.005	5.403
	C(2)-C(3)-C(4)	98.784	130.474	115.209	5.106
	C(3)-C(2)-C(1)	97.764	130.462	113.657	5.176

Docking site for 5VUX is represented in Figure 4.Two symmetrical potential binding sites corresponding to chain A and B were detected (binding site bs-1, with a volume of 662.016 Å³and surface of 1342.72Å² and bs-2, with a volume of 171.520 Å³ and a surface of 1176.32Å², respectively). The Cartesian coordinates are: for bs-1, a cube with origin at x =127.56 Å; y=250.39 Å and z=356.59 Å; cube side=40Å; for bs-2, a cube centered at x=107.00Å; y= 245.40Å; z=327.61Å; cube side=40Å. Coordinates are discussed for 5VUX chain A.



Fig 4:-Binding site of 5VUX corresponding to A and B chains: left- binding site colored by potential energy (chain B is represented as ball and stick); right- same binding site without protein chains showing only H2o atoms trapped in the binding surface.

Binding site 1 was considered for docking due to its larger size and correspondence with 7-(((4-(Dimethylamino)benzyl)amino)methyl)quinolin-2-amine binding site.

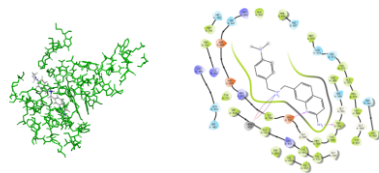


Fig 5:-(a) Human neuronal nitric synthase (nNOS) represented asball and sticks, in element colors, in the complex with 7-(((4-(Dimethylamino) benzyl) amino) methyl) quinolin-2-aminerepresented as space filling, in element colors; (b) 7-(((4-(Dimethylamino) benzyl) amino) methyl) quinolin-2-amine interaction with amino acids at nNOS binding site- (two hydrogen bonds are represented: GLI 597 and N atom; TRP 502 and NH₂ group; a salt bridge is also detected between NH⁺₂ and HEM 801.

12 best screened complexes ligand-5VUX are discussed below in figure 6

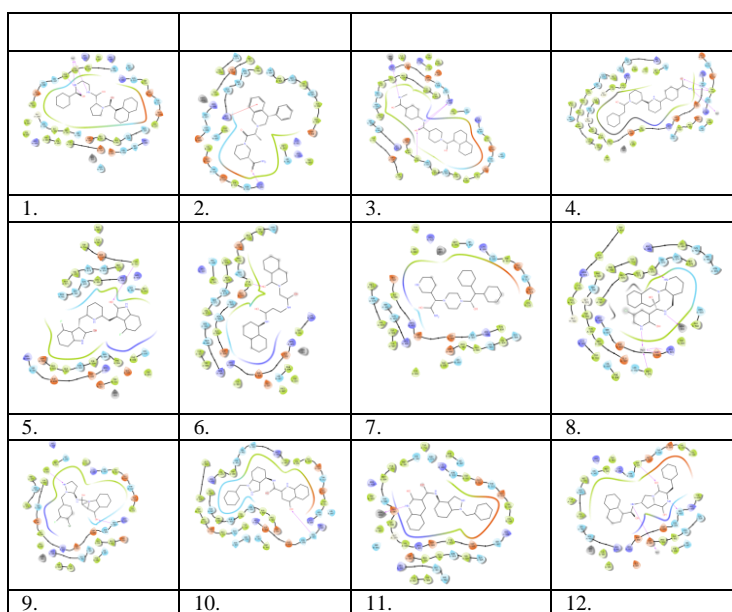


Fig 6:-First 12 compounds are shown docked at 5VUX binding site;hydrogen bounds are shown in pink;a 4Å off was used;1 H bond between Phe 696 and OH group, 2 H bound between Arg 486 and aromatic ring, H bonding Lys 309 and O; 3 H bound between Hem 801 and Nh group, Arg 608 and OH group, Arg 608 and NH, Ala 502 and OH ; 4 H bound between Trp 311 and OH, Trp 311 and NH₂; 5 H bound between Tyr 711 and OH; 6 H bound between Tyr 711 and OH group; 7 no H bound detected computationally; 8 H bound between Hem 801 and NH, Val 572 and NH; 9 H bound between Trp 683 and NH, Ser 607 and OH; 10 H bound between Ser 607 and OH; 11 H bound between Hem 801 and NH; 12 H bound between Ser 607 and NH, Asp 500 and NH, Trp 311 and OH.

Table 5 Screening results of the compounds Ba-computed binding affinity, IC₅₀ predicted –predicted values for IC₅₀ by the QSAR model.

Compounds	Ba	IC ₅₀ predicted
1	-12.952	-1.47503
2	-12.655	-1.47563
3	-12.448	-1.47583
4	-12.355	-1.47603
5	-12.336	-1.47623
6	-12.287	-1.47629
7	-12.235	-1.47689
8	-12.183	-1.47745
9	-12.172	-1.47802
10	-12.153	-1.47587
11	-12.115	-0.36312
12	-12.074	-0.3632
13	-12.067	-0.36357
14	-12.06	-0.3639
15	-12.057	-0.36402
16	-12.045	-0.36438
17	-12.044	-0.36539
18	-11.992	-0.36589
19	-11.968	-0.36609
20	-11.96	18.4646
21	-11.949	18.4683
22	-11.948	18.4697
23	-11.943	18.46702
24	-11.938	18.46734
25	-11.931	18.46756
26	-11.928	18.46789
27	-11.913	18.46812
28	-11.91	18.46833
29	-11.889	18.46853
30	-11.888	18.46879
31	-11.885	18.4689
32	-11.874	18.46902
33	-11.859	20.7806
34	-11.852	20.7816
35	-11.842	20.7823
36	-11.839	20.7837
37	-11.838	20.7836
38	-11.836	20.7899
39	-11.822	20.7902
40	-11.82	20.7946
41	-11.82	20.797
42	-11.818	20.7976

Compounds similarity score for active inactive and screening resulted compounds is represented in figure 7. At „ efficient” IC₅₀ it is notice that inactive and active compounds have similar structures.

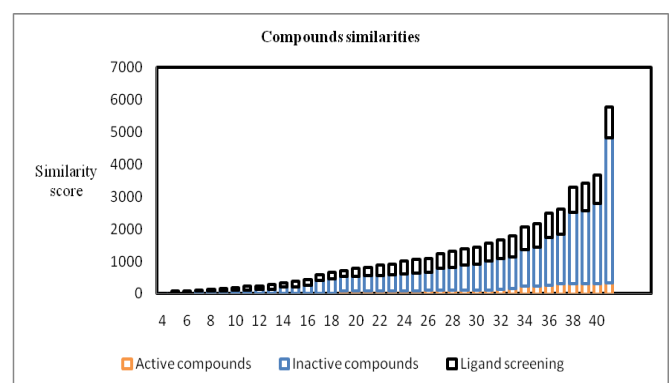


Fig 7:- Similarity scatter plot for active, inactive and screening resulted compounds.

IV. CONCLUSION

Based on *Inula* ssp. compounds, a valid pharmacophore hypothesis was computed. Novel compounds with potential inhibitory properties on Human neuronal nitric synthase were found. Neural network regression based on *Inula* ssp. compounds predicted IC₅₀ of the new screening resulted compounds. Hydrogen acceptor groups and carbonyl groups seems to be crucial in inhibiting nNOS. Presence of two hydrogen accepting group is also needed.

REFERENCES

- [1]. Cauwels A, Nitric oxide in shock, *Kidney Int*, 2007, 72(5), 557-565
- [2]. Pokidyshev DA, Bondarenko NA, Malyshev I et al. [Selective inhibition of inducible NO-synthase by nonselective inhibitor]. *Russ. Fiziol. Zh. Im. IM Sechenova*. 84(12), 1420–1427 (1998).
- [3]. Shahrestani P, Mueller LD, Rose MR. Does aging stop? *Curr Aging Sci* 2009; 2(1): 3-11. Banach M, Piskorska B, Czuczwar Sj, Borowicz KK. Nitric oxide, epileptic seizures, and action of antiepileptic drugs. *CNS Neurol. Disord. Drug Targets* 10(7), 808–819 (2011)
- [4]. Sullivan R, Graham CH. Chemosensitization of cancer by nitric oxide. *Curr. Pharm. Design* 14(11), 1113–1123 (2008).
- [5]. Rosenfeld, R.J., Garcin, E.D., Panda, K., Andersson, G., Aberg, A., Wallace, A.V., Morris, G.M., Olson, A.J., Stuehr, D.J., Tainer, J.A., Getzoff, E.D., Conformational Changes in Nitric Oxide Synthases Induced by Chlorzoxazone and Nitroindazoles: Crystallographic and Computational Analyses of Inhibitor Potency, (2002) *Biochemistry* 41: 13915-13925
- [6]. Elizabeth Igne Ferreira and Ricardo Augusto Massarico Serafim1, Nitric Oxide Synthase Inhibitors, *Biochemistry, Genetics and Molecular Biology* chapter 12 , ISBN 978-953-51-3164-9.
- [7]. Weiwen Jiang, Charles F.Reich III, David S.Pisetsky, Mechanisms of activation of the RAW264.7 macrophage cell line by transfected mammalian DNA, *Cellular Immunology* Volume 229, (1) 2004, 31-40.
- [8]. John J. Irwin and Brian K. Shoichet, ZINC – A Free Database of Commercially Available Compounds for Virtual Screening, *J Chem Inf Model*. 2005; 45(1): 177–182.
- [9]. Ben Cooke and Scott C. Schmidler Statistical Prediction and Molecular Dynamics Simulation *Biophys J*. 2008 Nov 15; 95(10): 4497–4511
- [10]. Hui Zhang, Ming-Li Xiang, Jun-Yu Liang, Tao Zeng, Xiao-Nuo Zhang, Ji Zhang, and Sheng-Yong Yang Combination of pharmacophore hypothesis, genetic function approximation model, and molecular docking to identify novel inhibitors of S6K1, *Mol Divers*. 2013; 17(4): 767–772.
- [11]. Harger, Matthew; Li, Daniel; Wang, Zhi; Dalby, Kevin; Lagardère, Louis; Piquemal, Jean-Philip; Ponder, Jay W.; Ren, Pengyu (2017). "Tinker-OpenMM : Absolute and Relative Alchemical Free Energies using AMOEBA on GPUs". *Journal of Computational Chemistry*. **38** (23): 2047–2055.
- [12]. EC Alexopoulos Introduction to Multivariate Regression Analysis *Hippokratia*. 2010 Dec; 14(Suppl 1): 23–28
- [13]. O'Brien, R. M. (2007). "A Caution Regarding Rules of Thumb for Variance Inflation Factors". *Quality & Quantity*. **41** (5): 673.
- [14]. Kutner, M. H.; Nachtsheim, C. J.; Neter, J. (2004). *Applied Linear Regression Models* (4th ed.). McGraw-Hill Irwi
- [15]. Takako Sakano, Md. Iqbal Mahamood, Takefumi Yamashita, and Hideaki Fujitani, Molecular dynamics analysis to evaluate docking pose prediction, *Biophys Physicobiol*. 2016; 13: 181–194.